Applied Catalysis B: Environmental 97 (2010) 299–306

Contents lists available at ScienceDirect

Applied Catalysis B: Environmental

journal homepage: www.elsevier.com/locate/apcatb

Selective production of olefins from bioethanol on HZSM-5 zeolite catalysts treated with NaOH

Ana G. Gayubo*, Ainhoa Alonso, Beatriz Valle, Andrés. T. Aguayo, Javier Bilbao

Chemical Engineering Department, University of the Basque Country, P.O. Box 644, 48080, Bilbao, Spain

ARTICLE INFO

Article history:
Received 9 February 2010
Received in revised form 14 April 2010
Accepted 17 April 2010
Available online 24 April 2010

Keywords:
Biorefinery
Bio-ethanol
HZSM-5 zeolite
Olefins
Deactivation
Hydrothermal stability

ABSTRACT

The behaviour of a HZSM-5 zeolite (SiO_2/Al_2O_3 = 30) in several time treatments with 0.2 M NaOH solution has been studied for the transformation of bioethanol into hydrocarbons in an isothermal fixed bed reactor and in the 225–425 °C range. A short treatment (for 10 min) decreases the acid strength of the sites from 135 kJ (mol of NH_3)$^{-1}$ to 125 kJ (mol of NH_3)$^{-1}$, which is effective for increasing the selectivity of propene and butenes and for attenuating the deactivation by coke. This catalyst allows obtaining a yield of 30 wt% of propene + butanes at 400 °C with 136 (g of catalyst) h (g ethanol)$^{-1}$ and a feed of ethanol/water with 5 wt% water. The operation in reaction–regeneration cycles can be carried out continuously without irreversible deactivation of the catalyst, which means not exceeding extreme conditions in the reaction step: 375 °C and 400 °C for water contents in the feed of 75 wt% and 5 wt%, respectively. More severe treatments decrease the hydrothermal stability of the zeolite.

1. Introduction

Biomass can be used as a solid fuel, or it can be converted by means of thermochemical and biochemical processes into liquid or gaseous form for the production of electric power, heat, chemicals, or gaseous and liquid fuels [1]. The bioethanol obtained from agricultural and forestry residues, energy crops and other forms of lignocellulosic biomass fulfils such requirements and results in net CO_2 reduction [2]. The main advantages of lignocellulosic biomass as raw material for obtaining bioethanol are its lower cost and having no relation to food products. Nevertheless, the industrial viability of fermentation requires solving certain difficulties, such as: (i) the development of microbial strains able to ferment sugars contained in both cellulose and hemicellulose with higher tolerance to ethanol, inhibitors and salts; (ii) process improvements aimed at energy saving, by integrating the saccharification and fermentation stages [3,4].

The progress expected in addressing these limitations in the medium term allows considering bioethanol as a short-term alternative to other oxygenates, such as methanol and DME (obtained by gasification) [5] and bio-oil (liquid product of flash pyrolysis) [6], which are also regarded as key intermediates for the production of fuels and raw materials from lignocellulosic biomass. The valorisation of these intermediates requires the introduction of new catalytic processes, although these intermediates can be treated at existing refinery units (MTO process reactors, FCC units or hydroprocessing units), which would considerably reduce capital assets [7,8].

The transformation of bioethanol into hydrocarbons (in particular C_3–C_4 olefins and BTXE aromatics) has attracted considerable interest for some time now [9–11], which has increased due to the demand for these products. The increasing demand for propene is due to the growth of polypropylene, acrolein and acrylic acid markets [12]. Butenes are used in the production of oxygenated additives and in alkylation and isomerization units [13]. Other interesting routes for the valorisation of bioethanol are the production of H_2 by steam reforming [14] and of ethyl acetate [15] and ETBE [16].

One advantage of the catalytic transformation of bioethanol, which is obtained with a mass content of ethanol of about 10%, is to reduce the severity of the distillation (ethanol–water system presents an azeotrope with 95% ethanol) and the subsequent and expensive dehydration technologies (separation with membranes, pervaporation) required for its use as automotive fuel [17].

The shape selectivity and moderate acid strength of the HZSM-5 zeolite are suitable for the transformation of bioethanol into ethene, C_3–C_4 olefins or higher hydrocarbons. The deactivation by coke is slower than in other materials with more severe shape selectivity in the porous structure, such as SAPO-34 [18] and LEV zeolite [19]. Ferreira Madeira et al. [20] have proven that, operating under conditions that enhance the production of liquid hydrocarbons (350 °C and 30 bar), deactivation for the HZSM-5 zeolite is lower

* Corresponding author. Tel.: +34 94 601 5449; fax: +34 94 601 3500.
E-mail address: anaguadalupe.gayubo@ehu.es (A.G. Gayubo).

0926-3373/$ – see front matter © 2010 Elsevier B.V. All rights reserved.
doi:10.1016/j.apcatb.2010.04.021

Nomenclature

d_p pore diameter (Å)
M_{ethene}, $M_{ethanol}$ molecular weight of ethene and ethanol ($kg\,mol^{-1}$)
$(m_{ethanol})_{inlet}$, $(m_{oxygenates})_{outlet}$ mass flow rate of ethanol at the reactor inlet and of oxygenates at the reactor outlet ($kg\,s^{-1}$)
$(m_{olefins})_{outlet}$ mass flow rate of C_2–C_4 olefins at the reactor outlet ($kg\,s^{-1}$)
$(m_{ethene})^e_{inlet}$ mass flow rate of ethene equivalent units contained in the feed ($kg\,s^{-1}$)
$(\overline{r_p})_i$ average production rate of product or lump i in the reaction step, Eq. (4) ((kg of lump i)(kg of catalyst)$^{-1}$ h^{-1})
S_{BET} BET surface area ($m^2\,g^{-1}$)
t time on stream (h)
V_{mesop}, V_{microp}, V_p mesopore, micropore and pore volume, respectively ($cm^3\,g^{-1}$)
$X_{ethanol}$ conversion of ethanol, Eq. (1)
Y_i yield of component or lump i, Eq. (2)

than for Hβ and HY zeolites, given that the micropore size of the latter is larger and their hydrogen transfer capacity is higher, which enhances coke formation. A fraction of the coke deposited on the HZSM-5 zeolite is deposited on the outside of the zeolite crystals, but Ferreira Madeira et al. [21] have proven that the formation of coke takes place mainly in the micropores, in which alkyl aromatic hydrocarbons occluding the zeolite structure have been found by IR spectroscopy. These intermediates have also been determined by Johansson et al. [22], who related these intermediates to the presence of the "hydrocarbon pool" mechanism in the transformation of bioethanol into hydrocarbons, similarly as has been established in the literature in the MTO process [23,24].

Ethene production from bioethanol with a high selectivity does not require high reaction temperatures, so that catalysts such as HZSM-5 zeolite with high Si/Al ratio do not have hydrothermal stability problems, even operating with high water contents in the feed [25]. However, the production of C_3–C_4 olefins and BTXE aromatics requires operating above 300 °C.

The role of water in the reaction medium is well documented in the transformation of methanol on HZSM-5 zeolites [26–28]. Nevertheless, scant attention has been paid in the transformation of bioethanol, although water is present in the feed into the reactor and is also formed in the dehydration of ethanol. Gayubo et al. [11] and Aguayo et al. [25,29] have proven that steam also attenuates the rates of the main reaction and coke deactivation in the transformation of bioethanol. These authors also determined that, above 400 °C and with a high content of water in the reaction medium, the HZSM-5 zeolite undergoes irreversible deactivation by dealumination, and activity is not recovered in the reaction–regeneration cycles. Consequently, the hydrothermal stability of the catalyst is a key factor for the viability of the process, in addition to the selectivity and minimization of the deactivation by coke. Song et al. [30] obtained a high yield of propylene (32%) at 500 °C, due to the cracking of higher hydrocarbons on a HZSM-5 zeolite catalyst of moderate acidity, but they do not study the regeneration of the catalyst. Makarfi et al. [31] have proven the existence of irreversible deactivation when HZSM-5 zeolite catalysts of different compositions (different Si/Al ratio, mechanical addition of gallium oxide and impregnation with zirconium oxide) used in the production of liquid hydrocarbons from bioethanol at 400 °C and under 1 atm and 3 atm are regenerated. The incorporation of 1 wt% of Ni gives a high hydrothermal stability to the HZSM-5 zeolite, which allows feeding bioethanol with 5 wt% water at 500 °C and with 75 wt% at 400 °C without irreversible deactivation problems [32]. Nevertheless, the hydrogenating activity of Ni generates a considerable yield of BTX aromatics.

It is well known in the production of olefins by transformation of oxygenates that the treatment of the HZSM-5 zeolite with a NaOH solution with a concentration below 0.2 M increases the amount of weak acid sites by decreasing the amount of strong acid sites. Simultaneously, it generates mesopores and increases the external surface of the zeolite crystals [33,34]. In this paper, catalysts prepared from HZSM-5 zeolites treated with NaOH have been used in the transformation of bioethanol into hydrocarbons in order to establish the treatment conditions of the zeolite and the operating conditions that allow achieving a high selectivity of propene and butanes and maintaining the hydrothermal stability of the catalyst, so that the operation under reaction–regeneration cycles can be carried out without irreversible deactivation.

2. Experimental

2.1. Reaction equipment and analysis

A reaction equipment provided with an isothermal fixed bed reactor has been used in line with a gas chromatograph (Hewlett Packard 6890 Series II) and a micro-GC (Varian CP) for product analysis. The equipment enables continuous operation under reaction–regeneration cycles, with time on stream sequences of the operating variables (such as temperature) in each one of the steps. The reactor is made of S-316 stainless steel with 9 mm internal diameter and 10 cm total effective length, placed within a stainless steel chamber heated by an electrical resistance. The bed is a mixture of catalyst and inert (sand calcined at 800 °C) in order to ensure isothermal operation and sufficient height to maintain plug flow at low space time conditions. The reaction and product analysis equipment and the operating methodology have been described in detail elsewhere [32,35].

2.2. Catalysts

The catalysts were prepared from a HZSM-5 zeolite (with SiO_2/Al_2O_3 ratio = 30), modified by alkaline treatment. The treatment consists in ion exchanging 10 g of commercial ZSM-5 zeolite (Zeolyst International) supplied in ammonium form with 300 ml of 0.2 M solution of NaOH (Panreac, R = 99%) in a polyethylene flask, by stirring at 80 °C for different times (10 min, 120 min and 300 min) using a reflux condenser connected to the flask to prevent evaporation. The concentration of 0.2 M for the NaOH solution is advisable for avoiding the dealumination of the zeolite [33,34].

After the specified exchange time, the mixture is removed from the hot bath and rapidly cooled using an ice bath. The separation of the solid phase obtained is carried out by screening using a filtering paper with a pore size of 0.8 μm. Firstly, the solid is dried for 24 h at room temperature and then at 110 °C for 24 h in an oven. In this way the zeolite exchanged with Na is obtained (ATX-ZSM-5), where X denotes the treatment time in min.

The zeolite is subsequently exchanged with a 1 M solution of $NH_4(NO_3)$ (Panreac, R = 98%) at 80 °C for 2 h with constant stirring, using a volume of solution approximately 10 times the weight of the zeolite. The solid is separated by filtration and this procedure is repeated. The zeolite is washed twice (for 2 h and 12 h) with distilled water at room temperature by stirring to remove the reagents. The solid is filtered and dried for 24 h at room temperature and then at 110 °C for another 24 h. The acid form is obtained after calcination (muffle Thermicon P Heraeous, SA) with the follow-

Table 1
Effect of the duration of the alkaline treatment on the physical properties of the zeolites and of the catalysts.

Zeolites	BET surface area,$m^2\ g^{-1}$	Mesopore volume,$cm^3\ g^{-1}$	Micropore volume (t-plot),$cm^3\ g^{-1}$	Micropore volume (HK),$cm^3\ g^{-1}$	Pore diameter (HK),Å
HZSM-5	364	0.12	0.09	0.16	5.3
AT10-HZSM-5	420	0.18	0.10	0.18	5.6
AT120-HZSM-5	372	0.25	0.09	0.17	5.4
AT300-HZSM-5	338	0.30	0.08	0.14	5.2

Catalysts	BET surface area,$m^2\ g^{-1}$	Mesopore volume,$cm^3\ g^{-1}$	Pore volume distribution (%)<20/20 < d_p (Å) < 500/>500	Solid density,$g\ cm^{-3}$
HZSM-5	267	0.65	4.5/41.4/54.1	1.79
AT10-HZSM-5	193	0.61	5.1/39.9/55.0	1.79
AT120-HZSM-5	182	0.53	4.8/37.1/58.1	1.78
AT300-HZSM-5	295	0.79	3.3/51.8/44.9	1.76

ing stages: ramp of 5 °C min^{-1} up to 400 °C; 3 h at 400 °C; ramp of 3.3 °C min^{-1} up to 450 °C; 16 h at 450 °C; ramp of 3.3 °C min^{-1} up to 550 °C; 3 h at 550 °C and cooling ramp of 4.4 °C min^{-1} to room temperature.

The active phase (ATX-HZSM-5) is subsequently agglomerated (by wet extrusion) with bentonite (Exaloid) and using alumina (Prolabo) calcined at 1000 °C as inert charge. The ratio of each component in the catalyst is 25 wt% of zeolite, 30 wt% of bentonite and 45 wt% of alumina. The agglomeration of the zeolite allows obtaining a catalyst with a particle size and mechanical resistance suitable for use in a fixed and/or fluidized bed, in order to obtain an ideal gas flow and minimize the attrition of particles. Furthermore, agglomeration generates a bentonite and alumina matrix with mesopores and macropores, which facilitates the diffusion of reaction components to the zeolite crystals and increases the thermal conductivity of the particle (these properties are very interesting for good dissipation of the heat generated in the combustion of the coke in the regeneration). Furthermore, the mesopores and macropores in the matrix are efficient for enhancing the location of the coke dragged to the outside of the pores, which attenuates the deactivation caused by pore blockage. Kim et al. [36] studied this attenuation of pore blockage in the HZSM-5 zeolite by generation of mesopores on the outside of zeolite crystal channels. Furthermore, runs carried out with particles made up of these materials have proven that bentonite and alumina (with a small acidity and very weak acid sites) have an insignificant activity in the transformation of bioethanol.

The drying of the extrudates is carried out at room temperature for 24 h, whereupon they are crushed and sieved to a particle diameter between 0.3 mm and 0.6 mm, dried at 110 °C for 24 h and calcined at 575 °C for 2 h, following a temperature ramp of 5 °C min^{-1}. Using the above conditions, a HZSM-5 zeolite without alkali treatment and its corresponding final catalyst have been prepared. Both have been studied as references.

The physical properties of the reference HZSM-5 zeolite, the zeolites treated with NaOH and those of the corresponding catalysts have been determined by N_2 adsorption–desorption (Micromeritics ASAP 2010) and by Hg porosimetry (Micromeritics Autopore 9220). Transmission Electron Microscopy images (TEM) (Philips CM200) have been obtained for the untreated HZSM-5 zeolite and after alkaline treatment. The crystallinity has been determined by X-ray diffraction analysis (Philips PW 1710).

Total acidity and acid strength distribution of the catalysts were determined by calorimetric measurement of the differential adsorption of NH_3 at 150 °C and subsequent temperature-programmed desorption (TPD) of adsorbed NH_3, with a ramp of 5 °C min^{-1} up to 550 °C. The equipment used was a thermobalance (SDT 2960, TA Instruments) connected on-line to a mass spectrometer (Thermostar, Balzers Instruments) [37,38].

After the kinetic runs, the coke content in the catalysts was determined by combustion with air in a thermobalance (SDT 2960, TA Instruments), connected on-line with a mass spectrometer (Thermostar, Balzers Instruments) and following an established protocol for the reproducibility of results [29,39].

3. Results

3.1. Catalyst properties

The physical properties of the reference HZSM-5 zeolite, of the zeolites treated with NaOH and of the corresponding catalysts are shown in Table 1. As observed, a short 10-min treatment increases the BET specific surface and the mesopore volume. The micropore volume of the zeolites increases slightly due to the formation of mesopores on the catalyst surface, which enhance the access to micropores that are difficult to reach in the untreated zeolite. However, longer treatments increase the volume of mesopores at the expense of the removal of the most superficial micropores and, consequently, the BET area decreases. A slight increase in mesopore volume is also observed when comparing the images of Transmission Electron Microscopy (TEM) for the untreated HZSM-5 zeolite and after a 300-min treatment (Fig. 1). In Fig. 1b, the mesopores created are small cavities that are identified by their whiter tonality in the zeolite crystals.

The pore volume distribution results of the different catalysts reveal that the matrix (bentonite and alumina) that dilutes the active phase (25 wt%) is the one that provides the catalysts with all the macropores and most of the mesopores. The surface area obtained for the catalyst prepared using the zeolite subjected to a very severe alkaline treatment (for 300 min, which is the longest in all the zeolites treated) may be due to the fact that this treatment enhances the dispersion of the treated zeolite in the matrix by reducing the agglomeration of zeolite crystals.

The X-ray diffraction analysis (Fig. 2) shows the loss of crystallinity of HZSM-5 with alkaline treatment, so the crystallinity is 87% after the 10 min treatment and 80% after 300 min.

The results of total acidity and acid strength distribution of the zeolites are shown in Fig. 3a. This figure shows that the alkaline treatment causes a slight decrease in total acidity, from 0.64 (mmol NH_3) (g zeolite)$^{-1}$ for the untreated zeolite to 0.51 (mmol NH_3) (g zeolite)$^{-1}$ for the AT300-HZSM-5 zeolite. The acid strength of the sites decreases noticeably from 135 kJ (mol of NH_3)$^{-1}$ for the untreated zeolite to 90 kJ (mol of NH_3)$^{-1}$ for the AT300-HZSM-5 zeolite.

The results of TPD of ammonia (Fig. 3b) are consistent with the previous ones. The temperature corresponding to the desorption peak of strong acid sites (which desorbs at higher temperature) decreases from 398 °C for the reference zeolite to 304 °C for the HZSM-5 zeolite subjected to 300 min of alkaline treatment. This temperature is only slightly higher than that corresponding to the peak of weak acid site desorption in the reference HZSM-5 zeolite (283 °C). The two graphs in Fig. 3 show that the alkaline treatment contributes to homogenizing the acid strength of the sites of the HZSM-5 zeolite.

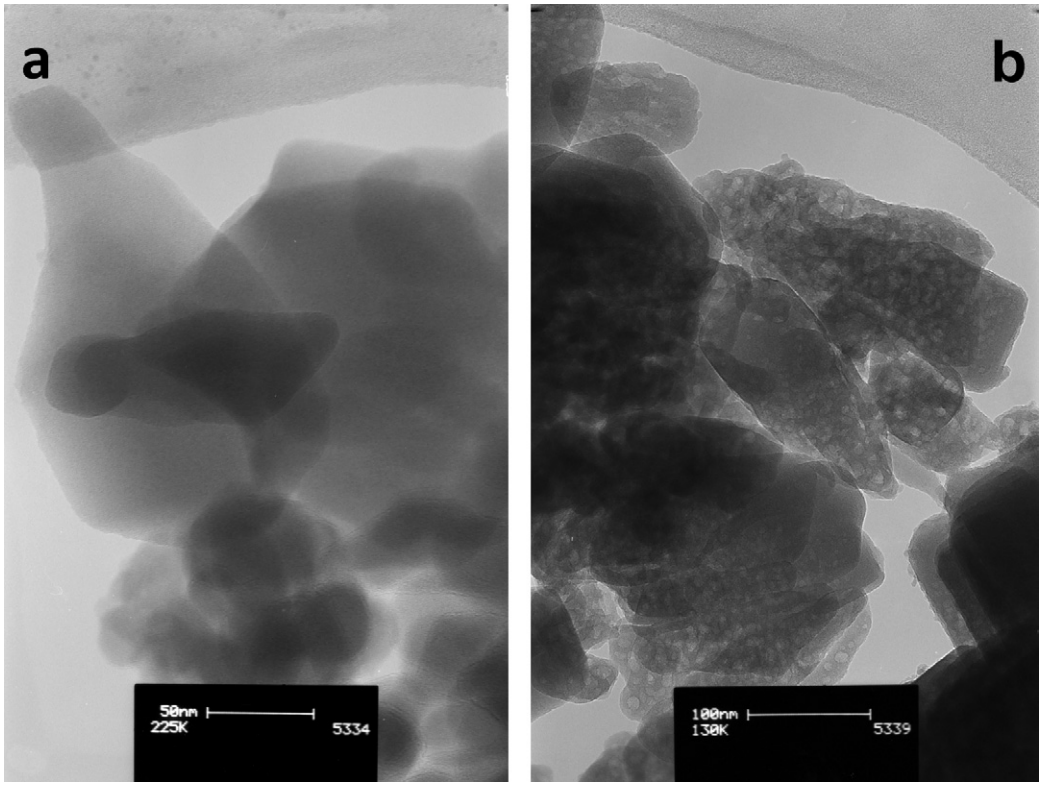

Fig. 1. TEM images for the HZSM-5 zeolite without treatment (graph a) and after treatment for 300 min with a NaOH solution (graph b).

3.2. Product yields and selectivities

A series of experiments with a temperature ramp of 0.7 °C min^{-1} have been carried out between 225 °C and 425 °C. The results in Fig. 4 correspond to the evolution with temperature of reactor outlet component concentration (ethanol, DEE, ethene, propene, butene, C_{4+} paraffins, olefins and aromatics C_{5+}). It is noteworthy that the experimentation following a temperature ramp facilitates kinetic result availability. Thus, operating under conditions in which the results are not masked by the deactivation and using a fast method for data analysis, only one run is required to obtain the evolution of conversion and yields with temperature. The concentration, X_i, is expressed as the fraction by mass unit of organic components in the reaction medium (excluding water).

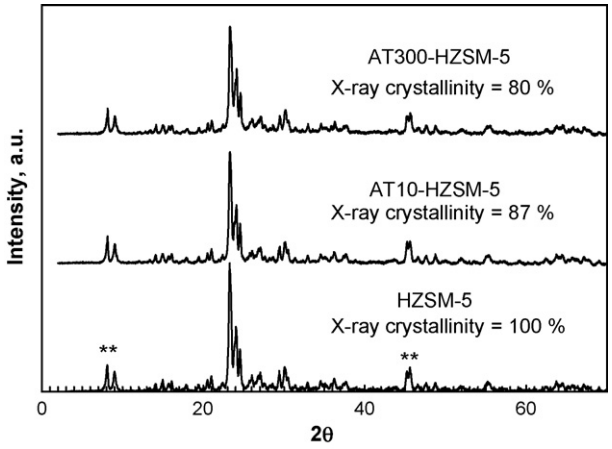

Fig. 2. XRD patterns of the untreated HZSM-5 zeolite and after treatment with NaOH solution for 10 min and 300 min.

The results show that at 225 °C the dehydration of ethanol is not complete, diethyl ether (DEE) being the main product of this dehydration, with a small concentration of ethene. The dehydration rate significantly increases above 245 °C, and ethanol conversion is complete at 270 °C for the catalysts prepared with the untreated HZSM-5 zeolite and with the AT10-HZSM-5 zeolite. This occurs at 285 °C for the catalyst based on the AT300-HZSM-5 zeolite, with ethene being the only product of the dehydration, which at these temperatures is also the major product. According to the literature [40], the dehydration of ethanol proceeds via the following steps: (i) adsorption of ethanol on a Brönsted acid site and formation of an oxonium ion with a partial positive charge on the ethanol oxygen and a partial negative charge on the oxygen bridge, (ii) ethoxy group formation, with elimination of a water molecule, and (iii) the ethoxy group releases ethene and another water molecule, and the Brönsted site is restored. The presence of ethoxy groups is detected by FTIR spectrometry [40,41].

Based on the results in Fig. 4, above 280 °C the reaction of ethanol dehydration to ethene is very fast and, using a HZSM-5 zeolite catalyst (of high acidity), a low value of space time is required for conversion to be complete in this step. Subsequently, ethene is transformed into higher hydrocarbons. The effect of temperature in Fig. 4 is similar to that observed in the literature with HZSM-5 zeolites [10,25].

The increase in temperature progressively favours the formation of propene and butenes, heavier aliphatic hydrocarbons (C_{5+} olefins and C_{4+} paraffins) and aromatics. Aromatic formation begins 20 °C above the temperature required for the formation of the other products.

This transformation of ethene evolves through oligomerization steps with carbocations as intermediates [42,43]. These carbocations are converted by cracking, isomerization, cyclization, aromatization and hydrogen transfer reactions, in which competition the acidity and shape selectivity of the catalyst and the

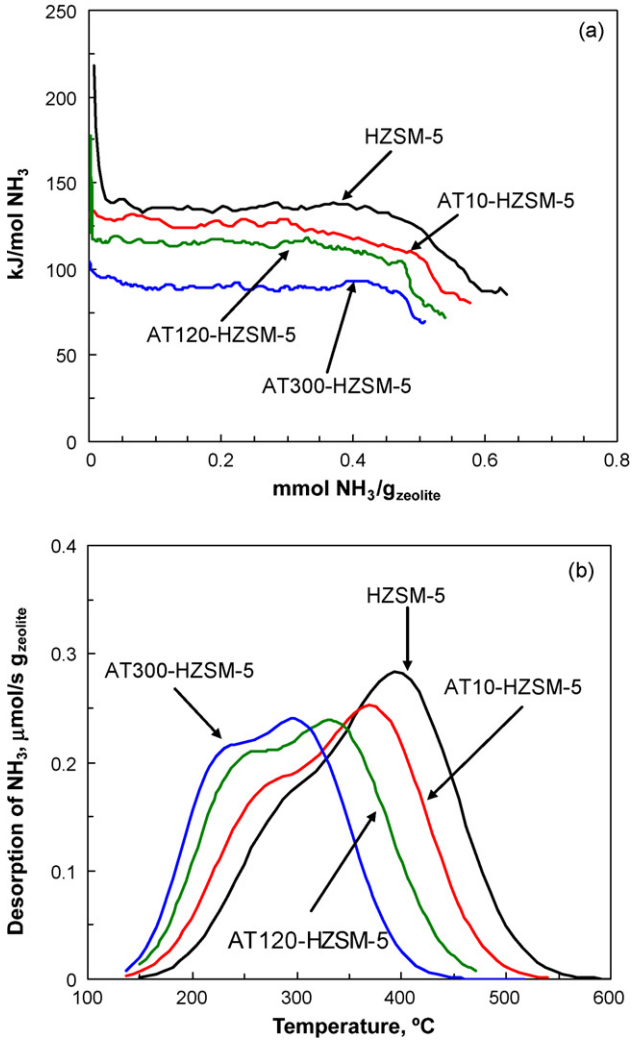

Fig. 3. Acid strength distribution (graph a) and TPD of ammonia (graph b) for the untreated HZSM-5 zeolite and after treatment with NaOH solution for different times.

operating conditions (especially temperature and water content in the reaction medium) play an important role. Based on the results in Fig. 4, propene precursors are all C_{4+} hydrocarbons, whose production is observed from temperatures at which significant propene is formed. The formation of butenes and C_{5+} olefins peaks around 335 °C for the catalyst with the untreated zeolite and at slightly higher temperatures for the catalysts prepared using treated zeolites. The C_{4+} paraffins and aromatics peak around 400 °C. Above this temperature the concentration of ethene slightly increases since it is a product of cracking reactions. It should be noted that the concentration of propene increases by increasing temperature to the maximum value studied, 425 °C.

In Fig. 5 the effect of temperature on the conversion of ethanol, $X_{ethanol}$, and on the yield of C_2–C_4 olefins, $Y_{olefins}$, is shown. Ethanol conversion was determined from the mass flow rate of ethanol at the reactor inlet, $(m_{ethanol})_i$ and the mass flow rate of oxygenates (ethanol and DEE), $(m_{oxygenates})_o$, at the reactor outlet:

$$X_{ethanol} = \frac{(m_{ethanol})_{inlet} - (m_{oxygenates})_{outlet}}{(m_{ethanol})_{inlet}} \quad (1)$$

The yield of C_2–C_4 olefins is calculated as the ratio between their mass flow rate at the reactor outlet, $(m_{olefins})_{outlet}$, and the mass flow rate of ethene equivalent units contained in the feed, $(m_{ethene})^e_{inlet}$:

$$Y_{olefins} = \frac{(m_{olefins})_{outlet}}{(m_{ethene})^e_{inlet}} \quad (2)$$

where

$$(m_{ethene})^e_{inlet} = (m_{ethanol})_{inlet}\frac{M_{ethene}}{M_{ethanol}} \quad (3)$$

As shown in Fig. 5, conversion is complete above 280 °C with the three catalysts studied, and at this temperature the yield of C_2–C_4

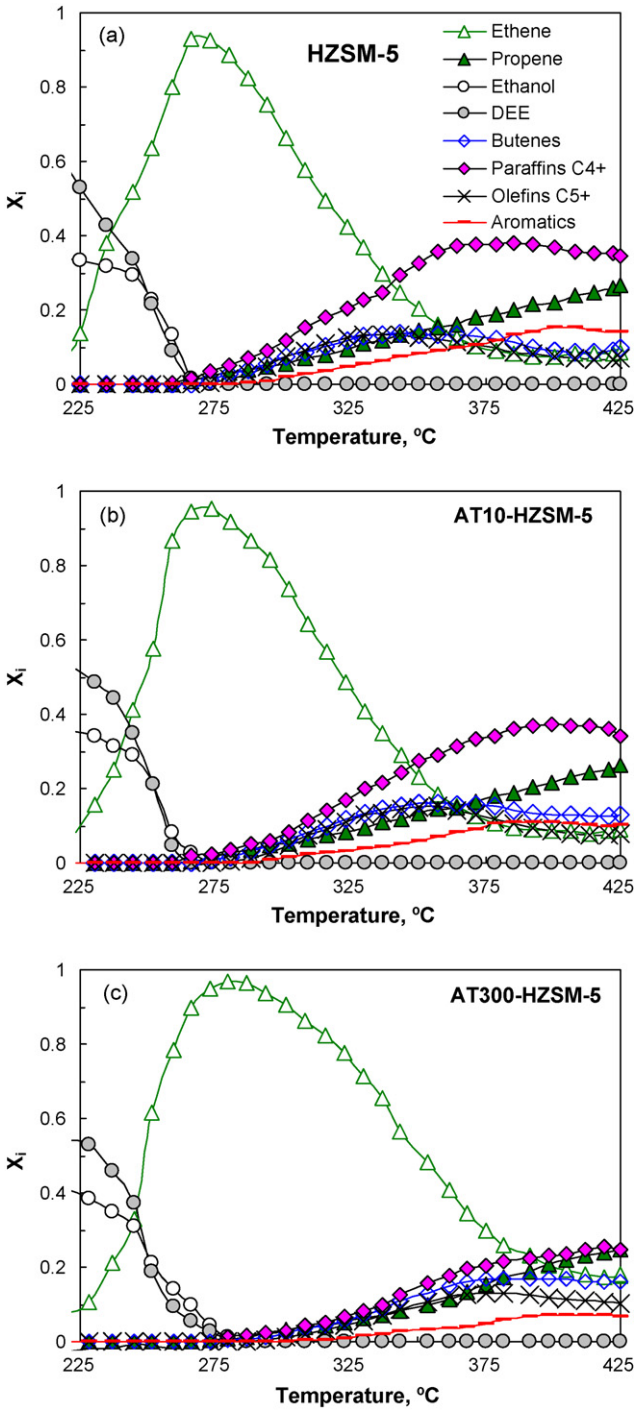

Fig. 4. Effect of temperature on product distribution at the reactor outlet at zero time on stream. Graph a, catalyst prepared with untreated HZSM-5 zeolite. Graph b, AT10-HZSM-5 catalyst. Graph c, AT300-HZSM-5 catalyst. Reaction conditions: feed, mass ratio of ethanol/water = 1; space time, 0.463 (g of catalyst) h (g ethanol)$^{-1}$.

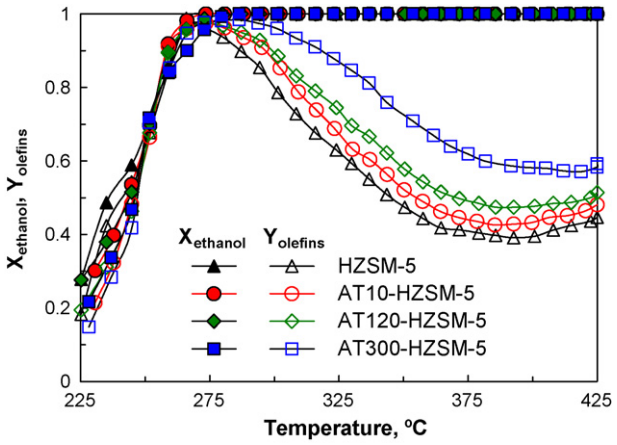

Fig. 5. Comparison of the effect of temperature on ethanol conversion and C_2–C_4 olefin yield for different catalysts. Reaction conditions: feed, mass ratio of ethanol/water = 1; space time, 0.463 (g of catalyst) h (g ethanol)$^{-1}$.

olefins is higher than 95 wt%. As temperature is increased above 280 °C the yield of olefins decreases as a result of the formation of other hydrocarbons and, above 400 °C, it increases due to the formation of ethene and propene by cracking. It should be noted that in the 280–425 °C range the maximum yield of olefins corresponds to the catalyst prepared with the HZSM-5 zeolite subjected to the most severe alkaline treatment (300 min).

The treatment of the zeolite with alkali has a marked effect on the distribution of products at zero time on stream, as shown in Fig. 6 corresponding to some of the experimental conditions taken as an example. A higher severity in the treatment with alkali (up to 120 min) leads to an increase in the concentration of ethene, propene + butenes and C_{5+} hydrocarbons, and a decrease in the concentration of C_1–C_4 paraffins and aromatics. The results for the treatment with alkali for up to 300 min (not shown here) follow the same trend. Based on the effect of the alkaline treatment on the physical properties (Table 1) and on the catalyst acidity (Fig. 3), and also on product distribution (Fig. 6), it is concluded that the more significant effect of this treatment is the attenuation of catalyst acidity, given that acidity decrease attenuates the steps of transformation of ethylene into higher hydrocarbons [20].

3.3. Deactivation

As a consequence of catalyst deactivation, the concentration of ethene increases with time on stream and the concentration of the other olefins decreases for all the catalysts. However, the effect of the treatment with alkali on catalyst deactivation is relevant. For a quantitative comparison, the values of the average rate of production of the different products for the different catalysts are compared in Fig. 7. These values have been calculated for 22 h of time on stream, as:

$$\left(\overline{r_p}\right)_i = \frac{(1/t)\int_0^t Y_i dt}{W/(m_{ethene})^e_{inlet}} \quad (4)$$

In Eq. (4) the yield of each lump of products, Y_i, is calculated as described above for the yield of olefins (Eq. (2)).

Fig. 7 shows that the average rate of production of propene + butenes and C_{5+} hydrocarbons increases with alkaline treatment severity, whereas these rates for C_{4+} paraffins and aromatics decrease. The results for the treatment with alkali for up to 300 min (not shown here) follow the same trend. The factors that contribute to this result are (i) the moderation of the acid strength (Fig. 3), which has a well-reported attenuating effect on deactivation by coke, and (ii) the increase in the mesoporosity, which, on the one hand, favours the diffusion of coke precursors to the outside of the zeolite crystals but, on the other, enhances the growth of coke polyaromatic structures [44–47]. The coke content of the deactivated catalyst in the runs shown in Fig. 7 is: HZSM-5 catalyst, 1.9 wt%; AT10-HZSM-5, 1.7 wt%; AT120-HZSM-5, 2.6 wt%, and AT300-HZSM-5, 3.4 wt%, which shows that a moderate treatment (10 min) is effective in attenuating the deposition of coke, which is attributed to the moderation of the acid strength of the treated zeolite (125 kJ (mol of NH_3)$^{-1}$ versus 135 kJ (mol of NH_3)$^{-1}$ of the untreated zeolite).

Inoue et al. [19] obtained a yield of 34.4% propene at 400 °C using a HLEV zeolite that undergoes a rapid deactivation by coke. Song et al. [30] obtained 32% of propene using a Zr-modified HZSM-5 zeolite that undergoes irreversible deactivation under the reaction conditions (500 °C). The yield of propene and butenes obtained in this paper using AT10-HZSM-5 catalyst is of 30 wt% at 400 °C and with a space time of 0.136 (g of catalyst) h (g of ethanol)$^{-1}$ and a bioethanol feed with the azeotropic composition. The advantage of this catalyst is the slow deactivation by coke for 22 h (the yield of propene + butenes is almost constant for this period) and the fact that there is no irreversible deactivation, as explained in the next section.

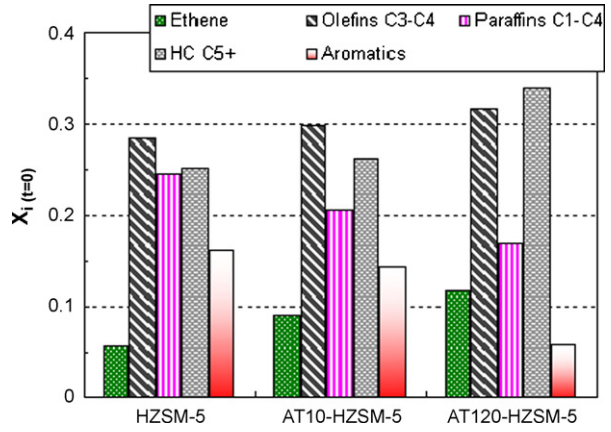

Fig. 6. Effect of the alkaline treatment duration on product composition at zero time on stream. Reaction conditions: feed, mass ratio of ethanol/water = 95/5; 400 °C; space time, 0.136 (g of catalyst) h (g ethanol)$^{-1}$.

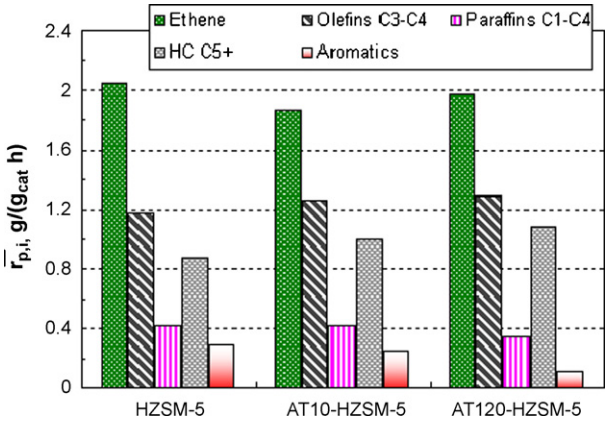

Fig. 7. Effect of the alkaline treatment duration on the average rate of production. Reaction conditions: feed, mass ratio of ethanol/water = 95/5; 400 °C; space time, 0.136 (g of catalyst) h (g ethanol)$^{-1}$; time on stream, 22 h.

3.4. Operation in reaction–regeneration cycles

The results in Fig. 8 show the evolution with time on stream of the mass fraction of ethene (by mass unit of organic components)

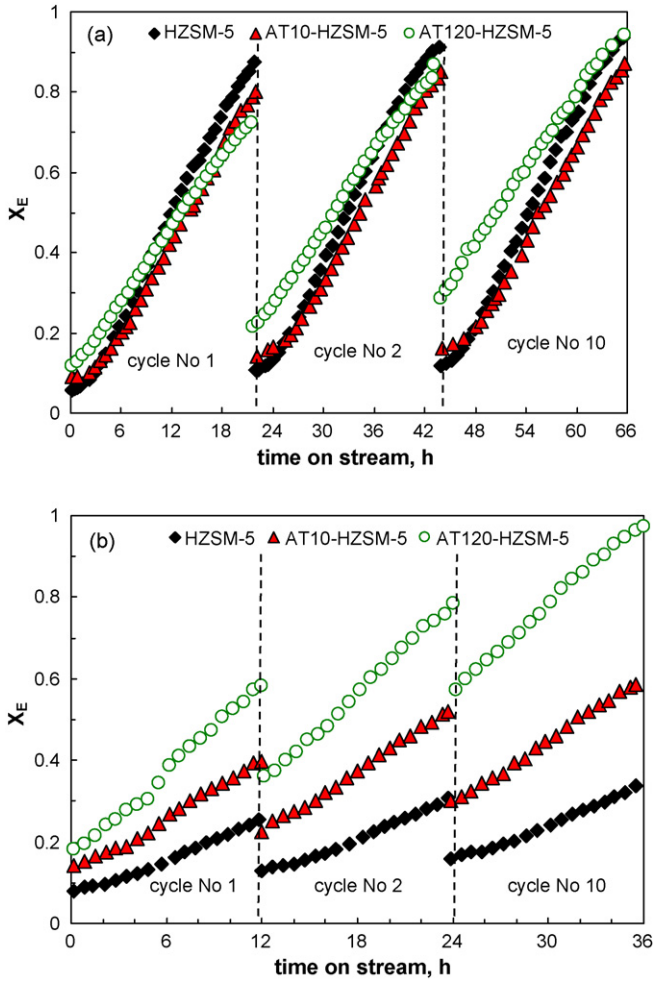

Fig. 8. Effect of the alkaline treatment duration on catalysts behaviour in reaction–regeneration cycles. Reaction conditions: 400 °C; Graph a, ethanol/water = 95/5 in mass, space time, 0.136 (g of catalyst) h (g ethanol)$^{-1}$. Graph b, ethanol/water = 1 in mass, space time, 0.235 (g of catalyst) h (g ethanol)$^{-1}$.

in experiments in successive cycles of reaction–regeneration (up to 10 cycles in Fig. 8a) carried out with the catalyst prepared using the untreated HZSM-5 zeolite and with the catalysts prepared using the zeolites treated with NaOH solution for 10 min (AT10-HZSM-5) and 120 min (AT120-HZSM-5). Each graph corresponds to a different water content in the feed. The remaining operating conditions are:

Reaction step: temperature, 400 °C, space time, 0.136 (g of catalyst) h (g of oxygenates)$^{-1}$ (graph a) and 0.235 (graph b).
Regeneration step: combustion of the coke deposited on the catalyst with air at 550 °C for 2 h.

Both steps are carried out *in situ* in the reactor and the aforementioned variables are previously established in the control software provided for automated reaction equipment [32,35].

Fig. 8a (for a feed with the azeotropic composition of the ethanol/water mixture) shows a slight reduction in catalyst activity after the first regeneration, but then the kinetic behaviour is maintained in the subsequent cycles for both the untreated zeolite and the zeolite treated for 10 min with NaOH solution. However, a longer treatment with alkali (for 120 min, catalyst AT120-HZSM-5) leads to a continuous reduction in catalyst activity in the successive cycles, which is due to the irreversible deactivation of the zeolite. The results for the treatment with alkali for up to 300 min (not shown here) follow the same trend.

The results of the successive cycles in Fig. 8b, corresponding to a feed with 50 wt% water, reveal a behaviour that is consistent with the irreversible deactivation of the three catalysts. Under these circumstances, activity steadily decreases in the successive reaction–regeneration cycles, although in a less pronounced way as the number of cycles is increased [48,49]. This reduction in activity is more evident for a longer treatment with alkali. It should be pointed out that the irreversible deactivation of HZSM-5 zeolite and the subsequent catalyst acidity deterioration are significant in the transformation of ethanol with water under conditions of lower reaction temperature and/or lower water content in the reaction medium than in the transformation of methanol to olefins [27,49]. The origin of this irreversible deactivation is the dealumination of the HZSM-5 zeolite [50,51].

4. Conclusions

The treatment of the HZSM-5 zeolite with 0.2 M NaOH solution is a simple technique that is effective for modifying the porous structure of the zeolite, by increasing its mesoporosity, and for moderating acid strength. A 10-min treatment is effective for the transformation of bioethanol in order to increase the selectivity of C_2–C_4 olefins, in particular that of propene and butenes, as a consequence of the zeolite acid strength attenuation to 125 kJ (mol of NH_3)$^{-1}$. This catalyst allows obtaining a yield of propene + butenes of 30 wt% at 400 °C and with a space time of 0.136 (g of catalyst) h (g of ethanol)$^{-1}$ and a bioethanol feed with the azeotropic composition. This yield remains almost constant for 22 h reaction. Longer treatments generate excessive mesoporosity, which promotes deactivation by coke deposition.

The HZSM-5 zeolite subjected to a mild treatment with alkali has a hydrothermal stability similar to that of the untreated zeolite. The limit for the reaction temperature can be set at 400 °C for a feed with a water content corresponding to the azeotropic mixture. Temperature has an important effect on the hydrothermal stability of the catalyst, so that at lower temperature the kinetic behaviour of the catalyst is reproducible in successive reaction–regeneration cycles with a water content in the reaction medium substantially higher than that of the azeotrope. Thus, it has been proven that reproducibility can be maintained at 375 °C, operating under reaction–regeneration cycles, with a water content in the feed up to 75 wt%.

In the 300–400 °C range it is possible to operate with high yields and selectivities of hydrocarbons, in particular of propene and butenes. Bioethanol conversion and product distribution depend on the operating conditions (temperature, space time), among which water content in the reaction medium has a significant role. This has a great influence on deactivation by coke and can affect the viability of the process. The complex dependence of the operating conditions requires further studies on kinetic modelling.

Acknowledgements

This work was carried out with the financial support of the Department of Education Universities and Research of the Basque Government (Project GIC07/24-IT-220-07) and of the Ministry of Science and Innovation of the Spanish Government (Project CTQ2006-12006/PPQ).

References

[1] A. Demirbas, Energy Convers. Manag. 50 (2009) 2239–2249.
[2] K.T. Tan, K.T. Lee, A.R. Mohamed, Energy Policy 36 (2008) 3360–3365.
[3] M. Balat, H. Balat, C. Öz, Prog. Energy Combust. Sci. 34 (2008) 551–573.
[4] O.J. Sánchez, A.C. Cardona, Bioresour. Technol. 99 (2008) 5270–5295.
[5] A.T. Aguayo, J. Ereña, D. Mier, J.M. Arandes, M. Olazar, J. Bilbao, Ind. Eng. Chem. Res. 46 (2007) 5522–5530.

[6] D. Mohan, C.U. Pittman, P.H. Steele, Energy Fuels 20 (2006) 848–889.
[7] A. Corma, G.W. Huber, L. Sauvanaud, P. OïConnor, J. Catal. 247 (2007) 307–327.
[8] M. Stöcker, Angew. Chem., Int. Ed. 48 (2008) 9200–9211.
[9] R. Le Van Mao, T.M. Nguyen, J. Yao, Appl. Catal. 61 (1990) 161–173.
[10] J. Schulz, F. Bandermann, Chem. Eng. Technol. 17 (1994) 179–186.
[11] A.G. Gayubo, A.M. Tarrío, A.T. Aguayo, M. Olazar, J. Bilbao, Ind. Eng. Chem. Res. 40 (2001) 3467–3474.
[12] D. Nakamura, Oil Gas J. 104 (2006) 56.
[13] G. Bellusi, P. Pollesel, Stud. Surf. Sci. Catal. 158 (2005) 1201–1212.
[14] W. Ni, D.Y.C. Leung, M.K.H. Leung, Int. J. Hydrogen Energy 32 (2007) 3238–3247.
[15] A.B. Gaspar, A.M.L. Esteves, F.M.T. Mendes, F.G. Barbosa, L.G. Appel, Appl. Catal. A: Gen. 363 (2009) 109–114.
[16] E. Weber de Menezes, R. Cataluña, Fuel Process. Technol. 89 (2008) 1148–1152.
[17] W. Kaminski, J. Marszalek, A. Ciolkowska, Chem. Eng. J. 135 (2008) 95–102.
[18] X. Zhang, R. Wang, X. Yang, F. Zhang, Micropor. Mesopor. Mater. 116 (2008) 210–215.
[19] T. Inoue, M. Itakura, H. Jon, Y. Oumi, A. Takahashi, Micropor. Mesopor. Mater. 122 (2009) 149–154.
[20] F. Ferreira Madeira, N.S. Gnep, P. Magnoux, S. Maury, N. Cadran, Appl. Catal. A: Gen. 367 (2009) 39–46.
[21] F. Ferreira Madeira, N.S. Gnep, P. Magnoux, H. Vezin, S. Maury, N. Cadran, Chem. Eng. J. (2010), doi:10.1016/j.cej.2010.01.026.
[22] R. Johansson, S.L. Hruby, J. Rass-Hansen, C.H. Christensen, Catal. Lett. 127 (2009) 1–6.
[23] M. Bjørgen, S. Svelle, F. Joensen, J. Nerlov, S. Kolboe, F. Bonino, L. Palumbo, S. Bordiga, U. Olsbye, J. Catal. 249 (2007) 195–207.
[24] S. Svelle, F. Joensen, J. Nerlov, U. Olsbye, K.P. Lillerud, S. Kolboe, M. Bjørgen, J. Am. Chem. Soc. 128 (2006) 14770–14771.
[25] A.T. Aguayo, A.G. Gayubo, A.M. Tarrío, A. Atutxa, J. Bilbao, J. Chem. Technol. Biotechnol. 77 (2002) 211–216.
[26] A.G. Gayubo, A.T. Aguayo, M. Castilla, M. Olazar, J. Bilbao, AIChE J. 48 (2002) 1561–1571.
[27] A.G. Gayubo, A.T. Aguayo, M. Olazar, R. Vivanco, J. Bilbao, Chem. Eng. Sci. 58 (2003) 5239–5249.
[28] A.G. Gayubo, A.T. Aguayo, A. Atutxa, R. Prieto, J. Bilbao, Ind. Eng. Chem. Res. 43 (2004) 5042–5048.
[29] A.T. Aguayo, A.G. Gayubo, A. Atutxa, M. Olazar, J. Bilbao, Ind. Eng. Chem. Res. 41 (2002) 4216–4224.
[30] Z. Song, A. Takahashi, N. Mimua, T. Fujitani, Catal. Lett. 131 (2009) 364–369.
[31] Y.I. Makarfi, M.S. Yakimova, A.S. Lermontov, V.I. Erofeev, L.M. Koval, V.F. Tretiyakov, Chem. Eng. J. 154 (2009) 396–400.
[32] A.G. Gayubo, A. Alonso, A.T. Aguayo, V. Valle, M. Olazar, J. Bilbao, Fuel (2009), doi:10.1016/j.fuel.2010.03.002.
[33] M. Ogura, S. Shinomiya, J. Tateno, Y. Nara, M. Nombra, E. Kikuchi, M. Matsukata, Chem. Lett. 8 (2000) 882–883.
[34] M. Ogura, S. Shinomiya, J. Tateno, Y. Nara, M. Nombra, E. Kikuchi, M. Matsukata, Appl. Catal. A: Gen. 219 (2001) 33–43.
[35] A.T. Aguayo, A.G. Gayubo, A. Atutxa, B. Valle, J. Bilbao, Catal. Today 107–108 (2005) 410–416.
[36] J. Kim, M. Choi, R. Ryoo, J. Catal. 269 (2010) 219–228.
[37] A.G. Gayubo, P.L. Benito, A.T. Aguayo, M. Olazar, J. Bilbao, J. Chem. Technol. Biotechnol. 65 (1996) 186–192.
[38] A.T. Aguayo, A.G. Gayubo, R. Vivanco, M. Olazar, J. Bilbao, Appl. Catal. A: Gen. 283 (2005) 197–207.
[39] J.M. Ortega, A.G. Gayubo, A.T. Aguayo, P.L. Benito, J. Bilbao, Ind. Eng. Chem. Res. 36 (1997) 60–66.
[40] J.N. Kondo, K. Ito, E. Yoda, F. Wakabayashi, K. Domen, J. Phys. Chem. B 109 (2005) 10969–10972.
[41] R. Barthos, A. Széchenyi, F. Solymosi, J. Phys. Chem. B 110 (2006) 21816–21825.
[42] S.A. Tabak, F.J. Krambeck, W.E. Garwood, AIChE J. 32 (1986) 1526–1531.
[43] P. Borges, R. Ramos Pinto, M.A.N.D.A. Lemos, F. Lemos, J.C. Védrine, E.G. Derouane, F. Ramôa Ribeiro, Appl. Catal. A: Gen. 324 (2007) 20–29.
[44] A.T. Aguayo, P.L. Benito, A.G. Gayubo, M. Olazar, J. Bilbao, Stud. Surf. Sci. Catal. 88 (1994) 567–572.
[45] M. Guisnet, P. Magnoux, Appl. Catal. A: Gen. 212 (2001) 83–96.
[46] H.S. Cerqueira, G. Caeiro, L. Costa, F. Ramôa Riberio, J. Mol. Catal. A: Chem. 292 (2007) 1–13.
[47] M. Guisnet, L. Costa, F. Ramôa Riberio, J. Mol. Catal. A: Chem. 305 (2009) 69–83.
[48] P.L. Benito, A.T. Aguayo, A.G. Gayubo, J. Bilbao, Ind. Eng. Chem. Res. 35 (1996) 2177–2182.
[49] B. Valle, A. Alonso, A. Atutxa, A.G. Gayubo, J. Bilbao, Catal. Today 106 (2005) 118–122.
[50] A. de Lucas, P. Cañizares, A. Durán, A. Carrero, Appl. Catal. A: Gen. 154 (1997) 221–240.
[51] T. Masuda, Y. Fujikata, S.R. Mukai, K. Hashimoto, Appl. Catal. A: Gen. 172 (1998) 73–83.